

Simplified Model of Interconnect Layers under a Spiral Inductor

Sonia M. Holik, Timothy D. Drysdale,

*Electronics Design Centre, Division of Electronics and Nanoscale Engineering, School of Engineering,
University of Glasgow, Glasgow, G12 8LT, United Kingdom,
e-mail: s.holik@elec.gla.ac.uk, tim.drysdale@glasgow.ac.uk*

Abstract— We demonstrate the feasibility of using effective medium theory to reduce the computational complexity of full-wave models of inductors that are placed over interconnects. Placing inductors over interconnects is one way that designers can tackle the problem of reducing overall chip size, however this has heretofore been a difficult option to evaluate because of the prohibitive memory requirements and run times for detailed simulations of the inductor. Here we replace the interconnects with a homogeneous equivalent layer that mimics their impact on the inductor to within 2% error, but reducing runtime and memory use by 90% or more.

Index Terms— Effective medium theory, interconnects, spiral inductor.

I. INTRODUCTION

In contemporary integrated circuits the on-chip inductors occupy a significant area. This limits the potential for down scaling the size of the chip, and has a concomitant cost implication. Since inductor sizes do not scale with process geometry, the problem is exacerbated, leading researchers to consider how the area underneath the inductor might be put to better use [1]. One option is to place interconnects underneath, but this raises difficulties with the simulation of the inductor. Simulation of the inductor is important because the three main parameters determining the performance of a spiral inductor, namely inductance, quality factor and self-resonant frequency, are influenced by the presence of nearby conductors. In contemporary CMOS technology dummy metal fill patterns are used to ensure the adequate metal density. The effect of specific dummy patterns on the inductor parameters where the metal fill is located on the same metal layer as the inductor, or underneath, has already been reported [2]-[4]. The influence of patterned ground shields has also been studied [5]-[8]. However more of these cases relate to the particular geometry, alignment and location of interconnect layers as would be found underneath an inductor. Specifically, interconnects are long narrow roads in which significant induced currents can occur, unlike dummy fills or patterned ground shield, that are designed to minimize such effects.

The particular difficulty in modeling an inductor located over an interconnect stack is large number of features that require to be meshed (leading to excessive memory usage) and also the large ratio between the wavelength (centimeters) and the sub-micron structure size that leads to numerical

inefficiencies in time-domain techniques [9]. Nonetheless, isolated structures can be solved given sufficient computational resource and time [10], or the analysis can be split into smaller segments [11]. Here we propose an alternative approach that deliberately exploits the mismatch in size between the wavelength and the structure, arising from earlier work in homogenizing interconnects [12]- [14]. We intend to demonstrate the feasibility of the approach by example, leaving a detailed development of a general method to future work.

II. SPIRAL INDUCTOR STRUCTURE

This section describes the structure of the exemplar spiral inductor studied in this paper as well as giving an overview of the homogenization process.

A. Numerical Model

A proprietary full vector 3D frequency domain electromagnetic solver tool was used throughout (HFSS) [15]. The exemplar conductor structure was designed to suit a conventional CMOS interconnection technology [16], [17]. We consider up to three layers of dense interconnects beneath the inductor. The interconnects layers are mutually perpendicular as it is shown in Fig. 1, with the top layout view of 7.5 turn rectangular spiral inductor of inner diameter $\alpha = 100 \mu\text{m}$, width $10 \mu\text{m}$ and spacing $2 \mu\text{m}$ in Fig. 1a, a perspective view of the spiral inductor with metal rods aligned in parallel on the mutually perpendicular metal layers underneath the inductor in Fig. 1b, and a cross section of the structure in Fig. 1c.

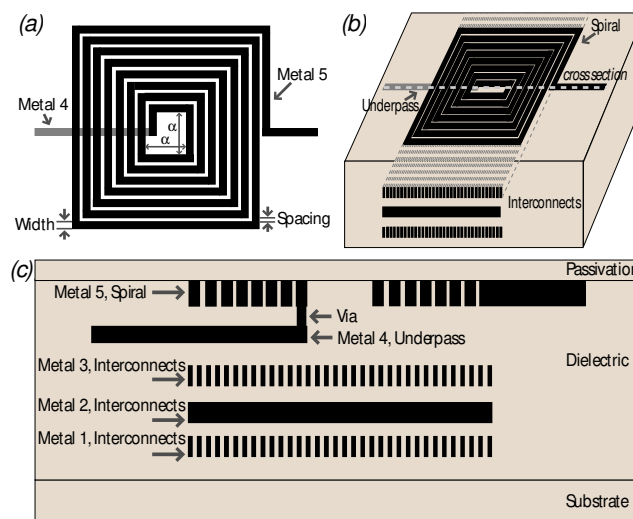


Fig. 1. The geometry of the spiral inductor: (a) top layout view of the rectangular spiral; (b) perspective view with metal rods underneath the spiral; (c) cross section of the structure.

The inductor is defined in the top most metal, Metal 5, a $1.1 \mu\text{m}$ thick layer of low conductivity aluminum $\sigma = 30 \times 10^6 \text{ S/m}$. The underpass at Metal 4 has thickness $0.75 \mu\text{m}$. The isolating silicon-oxide layer between Metal 4 and Metal 5 is $0.8 \mu\text{m}$ thick, while between Metal 3 and Metal 4, Metal 2 and Metal 3, Metal 1 and Metal 2, as well as Metal 1 and the substrate, it is $1 \mu\text{m}$ thick. The $1.1 \mu\text{m}$ thick interconnects are placed on Metal 1, Metal 2 and Metal 3, and are defined as electrically floating

metal (copper) rods not connected to the ground. The rods (330 elements on each metal layer) are aligned in parallel, and have length of 300 μm in order to cover the entire span of the inductor. The rods have width 0.45 μm and height 0.9 μm giving an aspect ratio of 2. The space between the rods is 0.45 μm , giving a metal fill factor of 0.5. The rods and inductor were modeled using layered impedance boundary conditions. The substrate is defined as 15 $\Omega\text{-cm}$ resistivity silicon of thickness 625 μm and is grounded by the perfect electric boundary conditions defined at the bottom plane, while other walls were defined as radiation boundaries. The spiral was covered by a 60 μm thick silicon-nitrate passivation layer.

B. Homogenization Approach

In order to homogenize the interconnect structure we use a modified Maxwell-Garnett (MG) mixing rule [12], [13] to calculate the effective permittivity of the homogeneous equivalent layer

$$\epsilon_{eff} = \epsilon_e + \Psi f \epsilon_e \frac{\epsilon_i - \epsilon_e}{\epsilon_i + 2\epsilon_e - f(\epsilon_i - \epsilon_e)} \quad (1)$$

where ϵ_i and ϵ_e are the dielectric functions of the inclusion and host material respectively (here, a metal and a dielectric), Ψ is a constant relating the fields inside and outside the inclusions (typically $\Psi = 3$ for spherical inclusions), f is the filling factor or ratio of the volume of the inclusion to the total size of the unit cell. The Maxwell-Garnett rule is known to give a qualitatively correct prediction of the effective properties of a composite with conducting inclusions [18]. The frequency dependant dielectric function of a metal inclusion ϵ_i is expressed by a Drude model [19].

III. NUMERICAL RESULTS

This section presents the obtained numerical results. First it shows the dependence of the performance of the inductor on the number of interconnect layers under the spiral. Further, the homogenization approach is numerically validated.

A. Interconnect Layers Dependence

It is well known that metal structures in the vicinity of inductors have an influence on their performance. Here we examine and demonstrate in Fig. 2 the relationship between the number of metal layers and inductor's parameters.

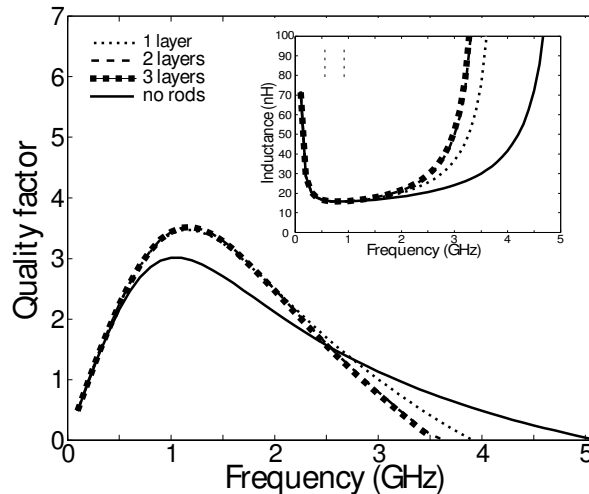


Fig. 2. The quality factor and inductance as a function of frequency for rectangular spiral inductor with various numbers of metal layers placed underneath the spiral.

Only the two topmost layers consisting mutually perpendicular metal rods under the inductor significantly changes the electromagnetic field and inductor's electrical characteristic. The reference structure defined as an inductor with no metal rods underneath has inductance of 16 nH, a maximum Q-factor of 3.04 at 1.1 GHz, and self-resonant frequency (SRF) of 5.1 GHz. When the entire area on Metal 3 was filled with metal rods the value and the frequency of the maximum Q-factor has change to 3.5 at 1.2 GHz, and the SRF dropped by 23% to 3.9 GHz. Further when the mutually perpendicular layer of metal rods was included on Metal 2 the maximum Q-factor remain the same but the SRF falls to 3.5 GHz (31%). Simulations indicate that including the third metal layer on Metal 1 or extending the interconnect stack by adding more metal layers (not shown here) does not significantly change the characteristic parameters of the inductor. This is because the parasitic capacitance is primarily determined by the two topmost metal layers. The inset plot of the inductance depicts that the SRF reduces with the different number of metal layers added underneath the spiral.

B. Homogeneous Equivalent Structure

In order to reduce the complexity of the model we replaced the layers of metal rods with a homogenous equivalent layer of the same thickness of 1.1 μm as the rods. In the empirical fitting procedure the linearly distributed values of the scaling factor Ψ were sampled within the interval of 1 to 10000 with the step increment of 100. For the particular geometry arrangement denser sampling of the values of Ψ does not reflect in notable change in the characteristic inductor's parameters. It was found that for the spiral inductor with one layer of metal rods underneath the fitted value of complex effective permittivity which gives good approximation of the characteristic parameters in the considered frequency range 1-8 GHz can be calculated from Eq. 1 with coefficient $\Psi = 900$ ($\epsilon_{\text{eff}} = 3604 + 9.5232 \times 10^{-4}i$). The results from the EMT simulation are compared against the detailed model in Fig. 3, illustrating good agreement (less than 2% error) for the frequencies below SRF, and

increased error up to 10% above SRF. Better approximation has been obtained for the structure with two layers of mutually perpendicular rods underneath the inductor. This indicates that an anisotropic homogenous equivalent layer may be required for the special case where interconnects are aligned along a single axis only.

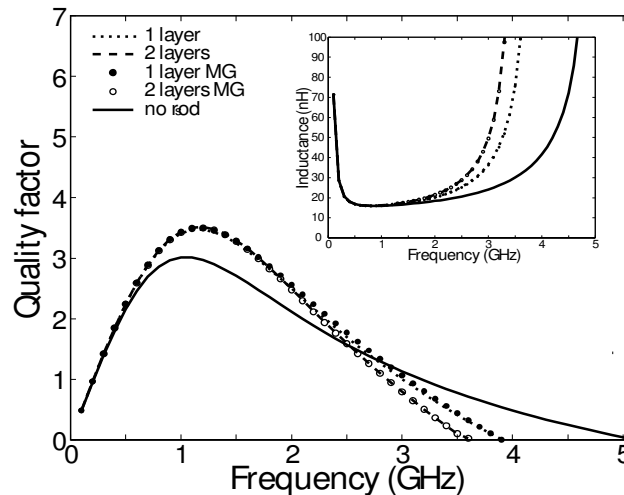


Fig. 3. The quality factor and inductance as a function of frequency for rectangular spiral inductor with one and two metal layers placed underneath the spiral. Results from homogenized equivalent structure are drawn as markers.

The empirically found value of $\epsilon_{eff} = 16004 + 4.2325 \times 10^{-3}i$ ($\Psi = 4000$) gives good agreement between the detailed and homogenized structure with an error less than 2% over entire frequency range. The value of Ψ and affiliated ϵ_{eff} is much higher than in the case of standalone structures [12], [13], and this corresponds to the change of the character of the illumination away from a plane wave. Also, in certain mixing ratios, mixtures with conductive constituents can have a larger value of the real part of ϵ_{eff} than either of the components [17].

Applying the EMT techniques reflects in significant reduction in computational time (69% for one layer and 95% for two layers under the inductor) and allocated memory (51% and 90% for one and two layers underneath, respectively). Regarding to the fact that only the two topmost layers of metal rods influence the change in inductor's parameters even higher reduction in computational time and allocated memory can be predicted for structures with additional interconnect layers. These promising results justify the displacement of further effort in obtaining more general results for the value of ϵ_{eff} for the range of structures designers are likely to account for.

IV. CONCLUSION

The numerical results presented in this paper show that multilayered interconnect structures with mutually perpendicular layers of parallel metal rods that are located underneath a spiral inductor can be replaced with a homogenous equivalent layer. The effective permittivity of this layer is calculated using the effective medium theory via a modified Maxwell-Garnett mixing rule. Using the homogenized equivalent layers, the simulations predict the values of quality factor and inductance

with an error of less than 2%, whilst reducing the runtime and memory usage by 90% or more. We expect that using a similar approach to our earlier work, empirical expressions can be developed to give the required fitting parameter across the range of inductor and interconnect structures that designers are likely to encounter, although we leave this significant effort to future work.

REFERENCES

- [1] F. Zhang, and P. R. Kinget, "Design of components and circuits underneath integrated inductors," *IEEE J. Solid-State Circuits*, vol. 41, no. 10, pp. 2265-2271, 2006.
- [2] J. H. Chang, Y. S. Youn, H. K. Yu, and C. K. Kim, "Effects of dummy patterns and substrate on spiral inductors for sub-micron RF ICs," *IEEE Radio Frequency Integrated Circuits Symposium, Digest of Technical Papers*, pp. 419-422, 2002.
- [3] C. L. Chen, "Effects of CMOS process fill patterns on spiral inductors," *Microwave and Optical Technology Letters*, vol. 36, no. 6, pp. 462-465, 2003.
- [4] H. M. Hsu, and M. M. Hsieh, "On-chip inductor above dummy metal patterns," *Solid State Electronics*, vol. 52, pp. 998-1001, 2008.
- [5] K. Murata, T. Hosaka, and Y. Sugimoto, "Effect of a ground shield of a silicon on-chip spiral inductor," *Proc. IEEE Microwave Conference*, pp. 177-180, 2000.
- [6] C. P. Yue, and S. S. Wong, "Design strategy of on-chip inductors for highly integrated RF systems," *Proc. IEEE Design Automation Conference*, pp. 982-987, 1999.
- [7] J. Chen, and J. J. Liou, "On-chip spiral inductors for RF applications: an overview," *J. Semiconductor Tech. Science*, vol. 4, no. 3, pp. 149-167, 2004.
- [8] X. Sun, G. Carchon, Y. Kita, K. Chiba, T. Tani, and W. De Raedt, "Experimental analysis of above-IC inductor performance with different patterned ground shield configurations and dummy metals", *Proc. 36th UMC'06*, pp. 40-43, 2006.
- [9] S. M. Holik, and T.D. Drysdale, "Simplified model of a layer of interconnects under a spiral inductor", accepted for publication in *Journal of Electromagnetic Analysis and Applications*.
- [10] J. Choi, M. Swaminathan, B. Beker, and R. Master, "Modeling of realistic on-chip power grid using FDTD method," *Proc. IEEE Int. Sym. Electromagnetic Compatibility*, vol. 1, pp. 238-243, 2001.
- [11] A. Fontanelli, "System-in-package technology: opportunities and challenges," *Proc. IEEE Int. Sym. Quality Electronic Design*, pp. 589-593, 2008.
- [12] S. M. Holik, and T. D. Drysdale, "Simplified model for on-chip interconnects in electromagnetic modeling of system-in-package," *Proc. 12th ICEAA'10*, pp. 541-544, 2010.
- [13] S. M. Holik, and T. D. Drysdale, "Effective medium approximation for electromagnetic compatibility analysis of integrated circuits," *Proc. 2nd ICAEMMO'08*, pp. 413-415, 2008.
- [14] S. M. Holik, T. D. Drysdale 'Simplified model of a layer of interconnects under a spiral inductor,' *J. Electromagnetic Analysis and Applications*, vol. 3, no. 6, pp. 187-190, 2011.
- [15] Ansoft High Frequency Structure Simulator (HFSS). <http://ansoft.com/>
- [16] M. Park, S. Lee, C. S. Kim, H. K. Yu, and K. S. Nam, "The detailed analysis of high Q CMOS-compatible microwave spiral inductors in silicon technology," *IEEE Trans. Electron Devices*, vol. 45, no. 9, pp. 1953-1959, 1998.
- [17] M. Park, G. H. Kim, J. Jang, J. G. Koo, and K. S. Nam, "Planarised interconnection technology using a new pillar formation method with multistacked metal structure," *Electron. Lett.*, vol. 32, no. 18, pp. 1731-1732, 1996.
- [18] A. Sihvola, , "Electromagnetic mixing formulas and applications," *IEE Publishing, London*, 1999.
- [19] J. B. Pendry, A. J. Holden, W. J. Stewart, and I. Youngs, "Extremely low frequency plasmons in metallic masostructures," *Physical Review Lett.*, vol. 76, no. 25, pp. 4773 – 4776, 1996.